⌘ *Author's Choice*

Polynucleotide Phosphorylase Activity May Be Modulated by Metabolites in *Escherichia coli*[*][S][◆]

Salima Nurmohamed[‡1], **Helen A. Vincent**[§1], **Christopher M. Titman**[‡], **Vidya Chandran**[‡], **Michael R. Pears**[‡], **Dijun Du**[‡], **Julian L. Griffin**[‡], **Anastasia J. Callaghan**[§2], **and Ben F. Luisi**[‡2]

From the ‡Department of Biochemistry, University of Cambridge, 80 Tennis Court Road, Cambridge CB2 1GA and §Biophysics Laboratories, School of Biological Sciences, Institute of Biomedical and Biomolecular Sciences, University of Portsmouth, Portsmouth PO1 2DY, United Kingdom

RNA turnover is an essential element of cellular homeostasis and response to environmental change. Whether the ribonucleases that mediate RNA turnover can respond to cellular metabolic status is an unresolved question. Here we present evidence that the Krebs cycle metabolite citrate affects the activity of *Escherichia coli* polynucleotide phosphorylase (PNPase) and, conversely, that cellular metabolism is affected widely by PNPase activity. An *E. coli* strain that requires PNPase for viability has suppressed growth in the presence of increased citrate concentration. Transcriptome analysis reveals a PNPase-mediated response to citrate, and PNPase deletion broadly impacts on the metabolome. *In vitro*, citrate directly binds and modulates PNPase activity, as predicted by crystallographic data. Binding of metal-chelated citrate in the active site at physiological concentrations appears to inhibit enzyme activity. However, metal-free citrate is bound at a vestigial active site, where it stimulates PNPase activity. Mutagenesis data confirmed a potential role of this vestigial site as an allosteric binding pocket that recognizes metal-free citrate. Collectively, these findings suggest that RNA degradative pathways communicate with central metabolism. This communication appears to be part of a feedback network that may contribute to global regulation of metabolism and cellular energy efficiency.

Ribonucleases play key roles in post-transcriptional regulation of gene expression in organisms from all domains of life. One well studied ribonuclease is polynucleotide phosphorylase (PNPase; E.C. 2.7.7.8),[3] a phosphorolytic exoribonuclease found in most bacteria as well as the eukaryotic organelles, the mitochondrion, and chloroplast (1, 2). In bacterial species PNPase affects complex processes, such as tissue invasive virulence of *Salmonella enterica* (3, 4) and the regulation of virulence secretion systems in *Yersinia* sp. (5). In *Escherichia coli*, PNPase contributes to the decay of bulk RNA, the quality control of ribosomal RNA, the turnover of small regulatory RNA, and cold shock response (1, 6–13).

A proportion of cellular PNPase is recruited into an RNA degrading machine, known as the degradosome, in *E. coli* and other γ-proteobacteria (14, 15). The degradosome is assembled upon an extensive scaffolding domain of the endoribonuclease RNase E (EC 3.1.26.12) (14, 16, 17); its other canonical components are the ATP-dependent DEAD-box RNA helicase RhlB (EC 3.6.4.13) and the glycolytic enzyme enolase (EC 4.2.1.11) (14, 15, 18). Small regions in the RNase E C-terminal domain mediate interactions with RNA (16) and with the cytoplasmic membrane to localize the degradosome assembly (19). This multienzyme complex provides a major contribution to RNA decay and, consequently, post-transcriptional gene regulation (20, 21).

Previous observations have hinted at a connection between RNA degradosome activity and central metabolism. The physical association of enolase, a glycolytic enzyme, with RNase E in the degradosome is required for response to phosphosugar stress (22). The importance of this interaction is highlighted by the observation that the recognition site for enolase is highly conserved in RNase E of γ-proteobacteria (23, 24). We have recently identified the Krebs cycle aconitase as a component of the RNase E-mediated RNA degradosome from *Caulobacter crescentus* (25). Although the Gram-positive bacterium *Bacillus subtilis* lacks an RNase E homologue, it has a functionally analogous ribonuclease (RNase J) that also interacts with glycolytic enzymes (26). The recurrence of stable interactions between ribonucleases and metabolic enzymes illustrates a remarkable evolutionary convergence that implies an important contribution of the interaction for organism fitness. Furthermore, the *E. coli* degradosome affects the abundance of transcripts encoding enzymes of central metabolism (20). Also suggestive of a link between RNA degradation and metabolism is the finding that PNPase activity can be regulated by nucleotides. *In vitro*, *E. coli* PNPase is allosterically inhibited by ATP (27), and its homologues from *Nonomuraea sp.* and *Streptomyces* are inhibited by the signaling molecule (p)ppGpp (28, 29). Although these observations implicate a communication between RNA degradative machines and central metabolism, evidence of such a linkage is missing.

Our earlier crystallographic studies of *E. coli* PNPase revealed the presence of citrate, originating from the crystallization buffer, at both the active site and at a "vestigial" active site,

which is related to the former through approximate molecular symmetry (30). These observations led us to explore whether citrate can affect the activity of *E. coli* PNPase *in vivo* and *in vitro*. Our data show that citrate influences PNPase activity in physiologically relevant concentration ranges. Our data also identify the vestigial active site of PNPase as a potential allosteric pocket that responds to metal-free citrate. Based on these findings, we propose a communication mechanism with feedback between RNA metabolism and central metabolism.

EXPERIMENTAL PROCEDURES

Ribonuclease Mutant Strain Growth Rate and Microarray Analyses

Ribonuclease null strains were provided by M. P. Deutscher (University of Miami). MG1655* I$^-$ (Δrna) in which the frameshift in the *rph* gene has been corrected was used as a parental control for the ribonuclease null strains; we will refer to this as wild-type throughout. MG1655* I$^-$ (Δrna), MG1655* I$^-$ PNP$^-$ (Δrna $\Delta pnp::kan$ Kan^R), a PNPase null strain, and MG1655* I$^-$ II$^-$ R$^-$ (Δrna $\Delta rnb::Tn10$ $\Delta rnr::kan$ Tet^{R}Kan^R), a RNase II/RNase R double null strain, were grown at 37 °C in M9-glucose in the presence or absence of 50 mM magnesium chloride, 50 mM sodium citrate. Doubling times were calculated from A_{600} measurements taken at 10-min intervals.

For global transcript analysis by microarray, wild-type MG1655* I$^-$ (Δrna) and PNPase null MG1655* I$^-$ PNP$^-$ (Δrna $\Delta pnp::kan$ Kan^R) strains were grown at 37 °C in M9-glucose to mid-exponential phase (A_{600} = 0.5–0.6). Cells were then grown at 37 °C for a further 30 min in the presence or absence of 50 mM magnesium chloride, 50 mM sodium citrate. Total RNA was extracted using the RNeasy RNA extraction kit (Qiagen) and analyzed using microarrays by Oxford Gene Technology, Oxford, UK.

Relative mRNA abundances were determined for the following experimental groups: (i) genes in the wild-type strain, MG1655* I$^-$, in the presence of citrate compared with the absence of citrate, (ii) genes in the PNPase null strain, MG1655* I$^-$ PNP$^-$, in the presence of citrate compared with the absence of citrate, and (iii) genes in the wild-type strain in the absence of citrate compared with the PNPase null strain in the absence of citrate. Only gene probes for which the raw intensity was greater than 100 were considered. Genes displaying a PNPase-mediated response to citrate were identified as those for which the effect of citrate was different by 2-fold or more in the PNPase null strain compared with the wild-type strain. Genes generally affected by PNPase were identified as those for which the relative mRNA abundance in the PNPase null was different by 2-fold or more relative to the wild-type strain. Gene Ontology terms as defined by the Gene Ontology website were assigned to each gene. The distribution among the Gene Ontology terms was compared for the genes displaying a PNPase-mediate response to citrate and those affected generally by PNPase.

Metabolome Analyses

Cells, Growth Conditions, and Sample Extraction—*E. coli* MC1061-derivative strains including PNPase parent, SVK29 (*pnp* null strain), AC21 (RNase E-parent), and AC27 (RNase E

lacking the last 477 residues from the C-terminal degradosome-scaffolding domain, *i.e.* a degradosome null strain) (31, 32) were provided by A. J. Carpousis (CNRS, Toulouse, France) and have a Tn10 marker linked to the *rne* allele. Strains were cultured at 37 °C in LB + antibiotic to an $A_{600} \sim 1$ and then harvested by centrifugation at 4200 $\times$ *g* at 4 °C for 20 min. Samples were recovered and stored at -80 °C. Metabolite samples were extracted using a methanol-chloroform method (33) to generate dried cell extract of the aqueous metabolites.

Metabolite Measurements by ^{1}H Nuclear Magnetic Resonance (NMR) Spectroscopy and Gas Phase Chromatography Mass Spectrometry (GC-MS)—Spectra were collected using a Bruker 500 MHz NMR spectrometer interfaced with a 5 mm TXI probe and processed using the ACD Labs one-dimensional NMR processor (ACD, Toronto, Canada) as previously described (34, 35). Dried aqueous extracts were derivatized before GC-MS as previously described (33). SIMCA-*p* + v.11.0 (Umetrics) was used for multivariate analysis. Data were processed using principal components analysis and partial least squares-discriminant analysis (PLS-DA). Details of these procedures are provided in the supplementary information.

Expression and Purification of PNPase Core

E. coli PNPase ΔKΔH1 (PNPase core) (36) was expressed using the auto-induction method (37) and purified as described previously (30).

Cloning, Overexpression, and Purification of PNPase and PNPase (R153A,R372A,R405A,R409A) Mutant

The *pnp* gene was generated by restriction digestion with NcoI and NotI from the pETDuet-1-*pnp-enol* (38). The pETDuet-1-*pnp* vector was constructed by subcloning the fragment of *pnp* bounded by NcoI and NotI into the multiple cloning site of expression vector pETDuet-1. The Arg-153 → Ala, Arg-372 → Ala, Arg-405 → Ala, and Arg-409 → Ala mutations were introduced into *pnp* using the QuikChange® site-directed mutagenesis method (Stratagene) with PCR primers PNPR153A_fw (5′-CCC GAT TGG TGC TGC CGC CGT AGG TTA CAT CAA T-3′) and PNPR153A_rev (5′-ATT GAT GTA ACC TAC GGC GGC AGC ACC AAT CGG G-3′), PNPR372A_fw (5′-CTT GAT GAA CTG ATG GGC GAA GCT ACC GAT ACC TTC CT-3′) and PNPR372A_rev (5′-AGG AAG GTA TCG GTA GCT TCG CCC ATC AGT TCA TCA AG-3′), and PNPR405A_R409A_fw (5′-GAA ATT GGT CAC GGT GCT CTG GCG AAG GCC GGC GTG C-3′) and PNPR405A_R409A_rev (5′-GCA CGC CGG CCT TCG CCA GAG CAC CGT GAC CAA TTT C-3′. The construct pETDuet-1-*pnp* was used as template for the site-directed mutagenesis experiments. The resulting construct pETDuet-*pnp(R153A,R372A,R405A,R409A)* was transformed into *E. coli* strain Rosetta (DE3). Cells were grown in an orbital shaker at 37 °C until the culture reached an absorbance at 600 nm of 0.5–0.6 and were then induced by the addition of 0.5 mM isopropyl 1-thio-β-D-galactopyranoside at 20 °C overnight. The cells were harvested by centrifugation, resuspended in lysis buffer (20 mM Tris, pH 8.0, 150 mM NaCl, 5 mM MgCl$_2$, 5 units/ml DNase I, 1 tablet/50 ml protease inhibitor mixture tablet), and lysed using a high pressure homogenizer (Emulsi-

flex). Cellular debris was removed by centrifugation at 31,500 rpm (SW32 Ti) for 30 min at 4 °C. PNPase(*R153A, R372A, R405A, R409A*) was precipitated from the supernatant by adding $(NH_4)_2SO_4$ to 51.3% saturation. The mixture was rotated at 4 °C for 1 h, and the pellet was collected by centrifugation at 22,000 rpm (SW32 Ti) for 20 min at 4 °C. The pellet was resuspended in buffer A (20 mM Tris pH 8.5, 30 mM NaCl, 5 mM $MgCl_2$, 5 mM DTT) and dialyzed against buffer A overnight. Sample was then loaded onto a HiTrap Q HP column and eluted with a linear gradient from 0 to 100% of the buffer A supplemented with 1 M NaCl. The fractions containing PNPase(*R153A,R372A,R405A,R409A*) were pooled, concentrated, and loaded onto a Sephacryl™ S500 HR XK 16/70 prep grade column equilibrated with GF buffer (20 mM Tris, pH 8.0,150 mM NaCl, 5 mM $MgCl_2$). Fractions containing purified PNPase(*R153A,R372A,R405A,R409A*) mutant protein were pooled and concentrated using a VIVA Spin column (molecular weight cutoff = 30 kDa). The PNPase parent was overexpressed and purified using the same procedure.

PNPase Activity Assays

Degradation Assay—The assay mix contained 0.05 mM poly(rA) 15-mer RNA, 10 mM $MnSO_4$ or $MgCl_2$, 10 mM phosphate, 20 mM Tris, pH 7.5, and 2 μM PNPase core with 0–20 mM sodium citrate. Assay samples were quenched with an equal volume of 200 mM EDTA at time 0 and 2 min after the addition of PNPase core. Assay samples (5 μl) were analyzed for RNA degradation by ion exchange HPLC (Dionex DNAPac 200 column, 25 °C, 0–1 M NaCl gradient in 20 mM Tris buffer pH 8.0 run over 8 min at 1 ml/min). Chromatograms were processed and analyzed in Dionex Chromeleon software.

Polymerization Assays—The assay mix contained 6.25 μM poly(rA) 15-mer RNA, 1 mM ADP, 20 mM Tris, pH 7.5, 1 mM $MgCl_2$ or 1 mM $MnSO_4$, 0–20 mM sodium citrate, and 2 μM PNPase. Five μl were quenched with an equal volume of 200 mM EDTA at time 0 and 1 min after the addition of PNPase core. Assay samples (5 μl) were analyzed for RNA polymerization by HPLC using the same conditions as for the degradation assay.

RESULTS

Citrate Affects PNPase Activity in Vivo—Whether PNPase activity is repressed by a metabolite *in vivo* can be evaluated by examining the impact of that metabolite on a strain that requires PNPase for viability. PNPase is essential in *E. coli* in the absence of either of the two other processive exoribonucleases, RNase II (39, 40) or RNase R (8, 41). A strain lacking RNase II and RNase R together is anticipated to be sensitive to the inhibition of PNPase activity because the double null mutants PNPase/RNase II (39, 40) and PNPase/RNase R (8, 41) are both inviable.

Within 30 min of adding magnesium-citrate to the culture medium, intracellular citrate levels increase significantly (supplemental Table S1). We observed that in the presence of 50 mM magnesium-citrate, an RNase II/RNase R double null mutant grew with a doubling time of 59.4 ± 3.2 min, compared with a doubling time of 49.0 ± 2.3 min in the absence of magnesium-citrate. In contrast, a PNPase null strain grew with similar dou-

bling times in the presence and absence of 50 mM magnesium-citrate (53.5 ± 2.2 min in the presence of magnesium-citrate and 54.3 ± 2.6 min in the absence of magnesium-citrate). These observations suggest that magnesium-citrate has a negative effect on an RNase II/RNase R double mutant, probably through inhibition of PNPase, which is required for viability in this strain. The parental strain was also insensitive to exogenously added magnesium-citrate, growing with a doubling time of 49.2 ± 1.9 min in the presence of 50 mM magnesium-citrate and a doubling time of 48.7 ± 2.6 min in its absence. This was not unexpected as this strain contains both RNases II and R, which could compensate for any loss in PNPase activity (8, 39–41).

Identification of Transcripts Impacted by PNPase-mediated Citrate Response—To identify transcripts that may be affected in a PNPase-mediated response to magnesium-citrate, we utilized gene expression microarray analyses. Comparison of the relative abundance of mRNAs revealed that 126 genes respond differently upon the addition of magnesium-citrate to the growth media in the parental strain compared with the PNPase null strain (Fig. 1*a*). Of those genes, roughly half were also sensitive to a loss of PNPase alone (the mRNA level of 655 genes was altered in the PNPase null strain relative to the parental strain grown on normal media), whereas the remaining portion was uniquely affected, suggesting an additional level of gene regulation by PNPase in response to magnesium-citrate.

The affected genes were clustered based on gene ontology (supplemental Table S2, a and b). The broad groups of functionally clustered genes that are affected by PNPase loss are similarly affected by the PNPase-mediated magnesium-citrate response (Fig. 1*b*). Closer inspection of the sub-groupings indicate that the PNPase-mediated magnesium-citrate response specifically affects transcripts of enzymes involved in processes of amino acid and derivative metabolism, cellular biosynthesis, and organic acid metabolism (Fig. 1*c*).

The relative abundance of *cirA*, *fkpA*, *gdhA*, and *rpoB* mRNAs in the PNPase null and wild-type strains in the presence of magnesium-citrate were explored by quantitative RT-PCR after rifampicin treatment to inhibit transcription. *cirA* and *fkpA* have previously been reported to be regulated by PNPase (10, 20). These transcripts were affected in a PNPase-mediated magnesium-citrate response in both our quantitative RT-PCR (supplemental Table S3) and microarray analyses. In contrast, the *gdhA* and *rpoB* transcripts were not significantly affected by a PNPase-mediated magnesium-citrate response by either quantitative RT-PCR (supplemental Table S3) or microarray. There are conflicting reports in the literature as to whether *gdhA* and *rpoB* transcripts are affected (20) or unaffected (10) by the absence of PNPase. Nonetheless, our results support the hypothesis that PNPase is involved either directly or indirectly in the response to changes in magnesium-citrate concentration *in vivo*.

PNPase Impacts the Metabolome—Having shown that the metabolite citrate may affect PNPase activity *in vivo*, we next investigated whether PNPase activity levels influence the cellular metabolome. Such an influence would enable a feedback loop that may regulate metabolite levels through their reciprocal impact on PNPase activity. Metabolite concentrations for a
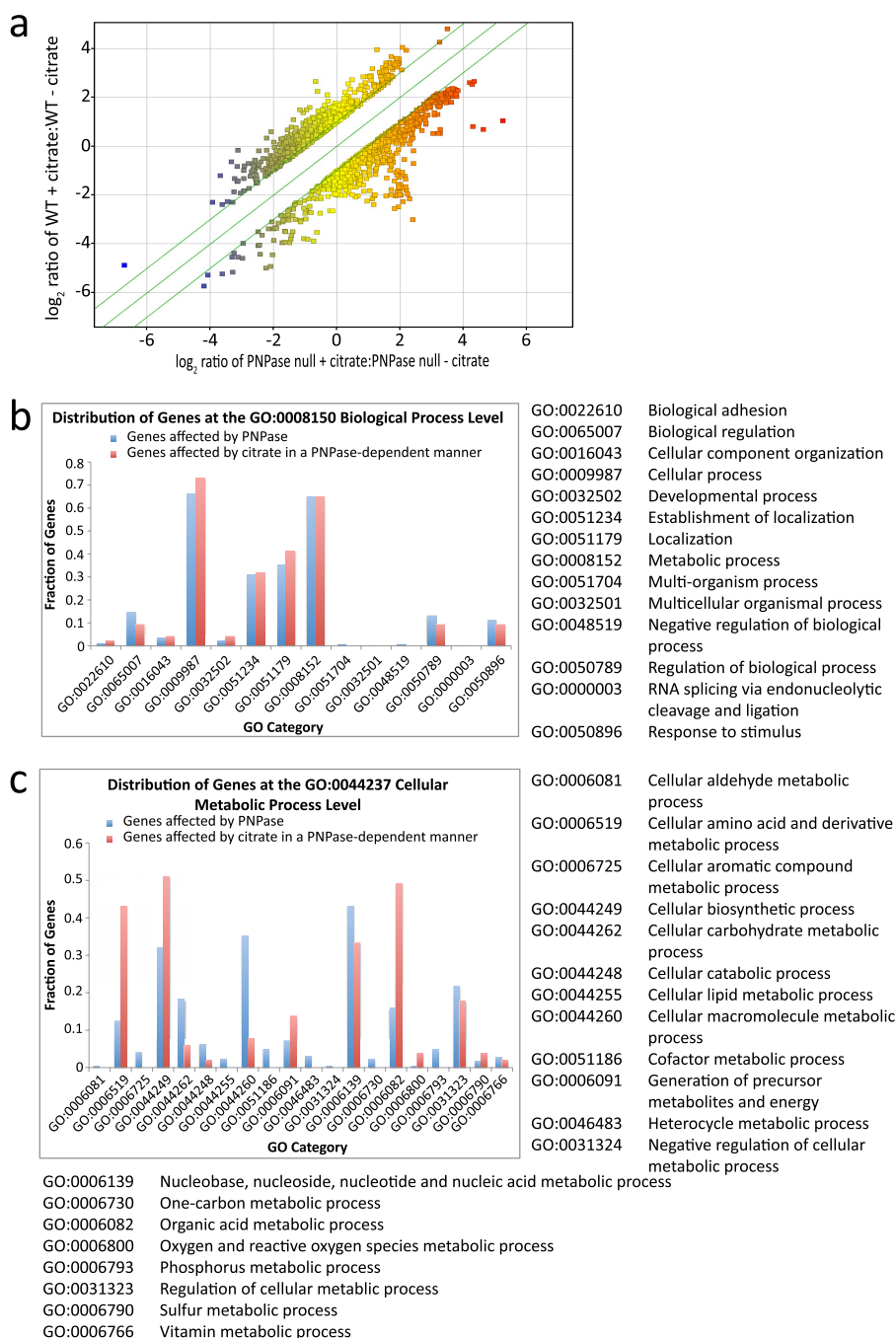
FIGURE 1. **The impact of citrate on global gene expression.** *a*, genes affected by citrate in a PNPase-dependent manner are shown. A plot of the $\log_2$ ratios for signal intensity for microarray probes in the presence of citrate relative to the absence of citrate for the wild-type strain *versus* the PNPase null strain is shown. This reflects the impact of citrate treatment on the relative mRNA abundance for the wild-type strain compared with the PNPase null mutant. Only shown are probes for which the relative abundance differs by 2-fold or more between the wild-type and PNPase null strain upon treatment with citrate. A single mRNA can be represented by multiple microarray probes. The data points are colored according to the *x* axis value (*blue* is negative, and *red* is positive) to aid visualization of individual points. *b*, the PNPase-mediated citrate response and PNPase ablation have a similar impact on gene expression. Genes affected by PNPase were determined by comparing the relative mRNA abundances that differ 2-fold or greater for the wild-type strain and a PNPase null strain in the absence of citrate. Genes affected by PNPase-mediated citrate response were determined as described in *a*. Groupings were made by Gene Ontology at the level of GO:0008150 Biological Process. *c*, PNPase-mediated citrate response broadly affects genes involved in cellular metabolic processes. Genes were grouped by Gene Ontology at the level of GO:0044237 Cellular Metabolic Process. In comparison to the genes that are affected by PNPase activity, those genes affected by citrate in a PNPase-dependent manner are involved more specifically with cellular amino acid and derivative metabolic processes, cellular biosynthetic processes, and organic acid metabolic processes than carbohydrate metabolic processes and cellular macromolecule metabolic processes.

PNPase null strain and the parental strain were determined by ^{1}H NMR spectroscopy and gas chromatography mass spectrometry. Many metabolites throughout central metabolism are affected by the loss of PNPase (supplemental Fig. S1). Notably, the Krebs cycle metabolite succinate decreases, whereas citrate concentrations increase, the latter possibly reflecting the disruption of a feedback loop.

Metabolite concentrations were also examined in a strain for which PNPase activity is uncoupled from the degradosome through the deletion of the C-terminal degradosome-scaffold-
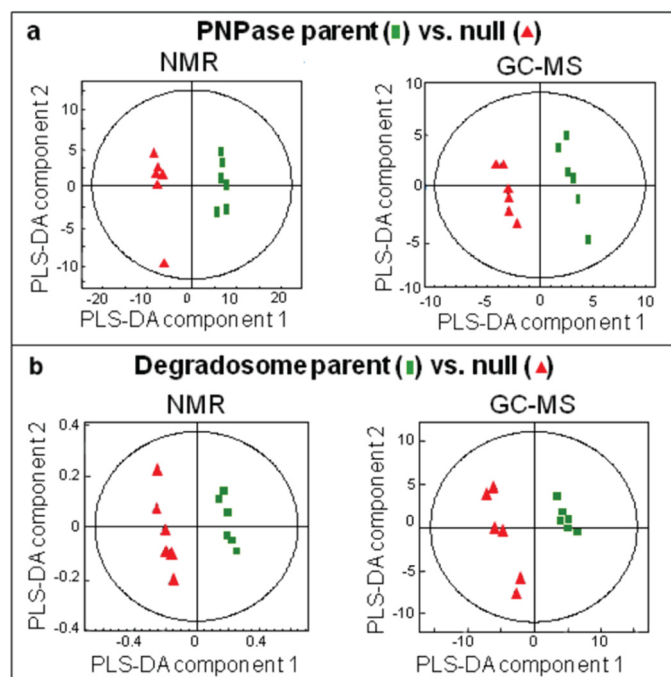
FIGURE 2. **Impact of PNPase and the degradosome on metabolism.** *a*, projection maps of the effects of PNPase deficiency on metabolic profiles with PLS-DA scores generated from PNPase parent (■) and null (▲) strains. A combination of high resolution ^{1}H NMR spectroscopy and GC-MS were used to provide coverage of the *E. coli* aqueous endometabolome. The distribution of extracted metabolites was analyzed by principal component analysis to examine the variation of metabolite concentration and composition within the dataset and PLS-DA to identify significant metabolite differences between the PNPase null and parental strains. The graph represents a two-dimensional projection map of PLS-DA scores generated from the multivariate analysis of the aqueous metabolites extracted from the respective parent (■) and null (▲) strains. This multivariate statistical technique correlates variables (metabolites or integral regions) with PLS-DA component 1, representing the dominant trend in the dataset, and PLS-DA component 2, representing the second largest amount of variation in the data. Each data point represents the pool of metabolites in each sample; the experiments were repeated six times. Plots are shown for extracts from cells grown in LB medium and analyzed by NMR (*left panel*) or GC-MS (*right panel*). R^2 and Q^2 values are 58 and 95% (NMR) and 46 and 84% (GC-MS), respectively. Typically a $Q^2 > 40\%$, calculated by cross-validation of every sixth sample iteratively, is indicative of a robust and predictive model. *b*, the degradosome affects on metabolism are shown. A projection map of the effects of degradosome deficiency on metabolic profiles is shown. PLS-DA scores plots were generated from the multivariate analysis of the aqueous metabolites extracted from the parent strain (■) and the degradosome deficient derivative (▲). Plots are shown for extracts from cells grown in LB medium and analyzed by NMR (*left panel*) or GC-MS (*right panel*). R^2 and Q^2 values are 47% and 95% (NMR) and 41%, 82% (GC-MS), respectively.

ing domain of RNase E (degradosome null). Compared with the parental strain, significant differences are distributed across many metabolic pathways, including the Krebs cycle, amino acid synthesis, and glycolysis (supplemental Table S4). Salient differences are seen for amino acids and increases in the concentrations of succinate, fumarate, and malate, suggesting uncoupling of the two halves of the Krebs cycle (supplemental Fig. S2).

The distribution of extracted metabolites may be represented graphically using principal components analysis to examine the variation of metabolite concentration and composition within the dataset and PLS-DA to identify significant metabolite differences between the null and parental strains. The projection maps in Fig. 2 are two-dimensional graphs of the dominant variations in the first two components of the

PLS-DA scores. These representations show that it is possible to distinguish on the basis of metabolite distributions the PNPase null from the parental strain (Fig. 2*a*) as well as the degradosome null and its parent (Fig. 2*b*).

Collectively, these findings suggest that PNPase and the degradosome have a wide-ranging impact on metabolism. In contrast, mutants lacking single enzymes of central metabolism are reported to have small metabolome changes due to re-routing of metabolic fluxes (42). The more global effects of RNA degradative machines on metabolism suggest that they potentially contribute to robust metabolic regulation.

Citrate Affects PNPase Activity in Vitro—The mechanism of communication between the metabolite citrate and PNPase could be indirect, direct, or a combination of both effects. We next sought to investigate if citrate can interact physically with PNPase and modulate its activity *in vitro*. We tested the impact of both free citrate and magnesium-citrate as *in vivo* citrate can exist in free- and magnesium-chelated forms.

We first tested whether citrate can bind directly at physiologically relevant concentrations to PNPase. Interaction of magnesium-citrate with PNPase could be detected using surface plasmon resonance, and the K_D was determined to be in the low mM range (supplemental Fig. S3a). This is in the same concentration range as our observed intracellular citrate concentrations for *E. coli* grown in minimal media (supplemental Table S1) and values previously reported (43) (1.2–4.4 mM in minimal media with glucose or glycerol as carbon source, increasing to 22 mM in acetate minimal media). The affinity of PNPase for free citrate is roughly 10-fold lower than the affinity for magnesium-citrate (supplemental Fig. S3b). It is possible that free citrate and magnesium-citrate bind PNPase at the same site with magnesium, significantly enhancing the interaction. Alternatively, the free citrate and magnesium-citrate may bind at distinct sites; from recent structural data, this appears to be the case (see below and PDB code 3GCM; Ref. 30).

Having demonstrated that citrate can bind directly to PNPase at physiological concentrations, we next investigated its effect on PNPase activity. Degradation of RNA by PNPase *in vitro* requires inorganic phosphate and the presence of divalent metal cation as a co-factor with 10 mM Mg^{2+} being optimal. In the presence of mM concentrations of citrate, conditions in which the citrate would be predominantly complexed as magnesium-citrate given the Mg^{2+} concentration, the degradative activity of PNPase is inhibited (Fig. 3, *a* and *b*). The observed inhibition was not solely due to loss of available metal co-factor, as citrate remains inhibitory in the presence of Mg^{2+} in a 2-fold excess over citrate (Fig. supplemental Fig. S4b; degradation is inhibited in the presence of 5 mM citrate, 10 mM Mg^{2+}). Furthermore, manganese can substitute for magnesium as the catalytic metal in PNPase, and RNA degradation was unaffected in the presence of mM concentrations of manganese and citrate. This suggests that the inhibition seen with magnesium-citrate requires a specific ligand geometry and is not due simply to sequestering the required metal cofactor (Fig. 3*b*).

In addition to its degradative role, PNPase can also function as a polymerase, adding 3′ tails to transcripts (1, 12). This reaction is the reverse of degradation and is favored when nucleoside diphosphate rather than inorganic phosphate is present in
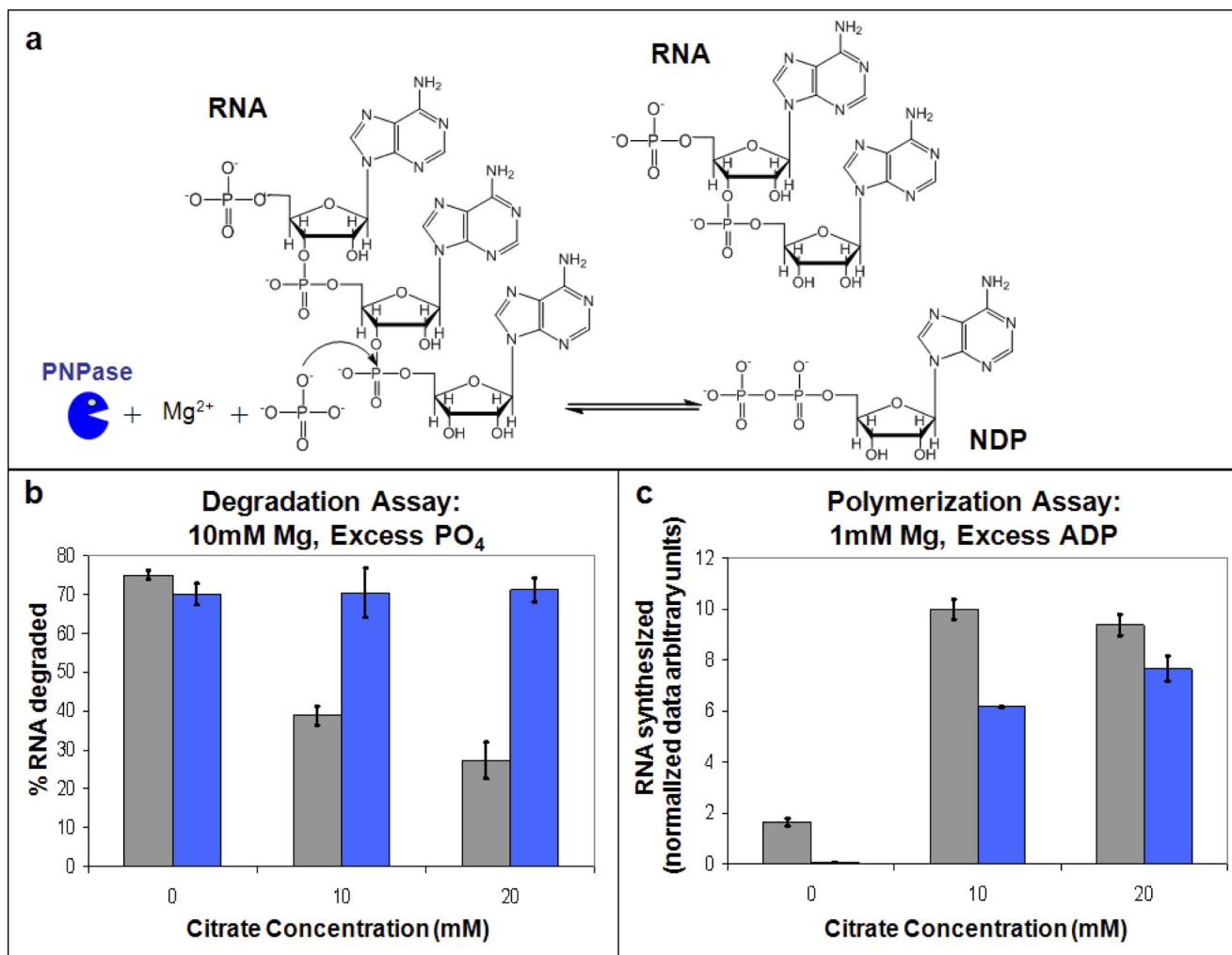
FIGURE 3. **Effect of citrate on the *in vitro* activity of PNPase.** *a*, shown is a schematic representation of the RNA degradation (forward) and polymerization (reverse) mechanisms of PNPase. Note that different experimental assay conditions are used to "switch" PNPase between RNA degradation and polymerization modes. *b* and *c*, analysis of PNPase core activity catalyzed by Mg^{2+} (*gray*) and Mn^{2+} (*blue*) in the presence of varying citrate concentrations is shown. Data represent experimental repeat averages with S.D. indicated by *bars*. *b*, a RNA degradation assay shows the amount of 15-mer RNA degraded as a percentage at the end of the assay period. *c*, RNA substrate-based polymerization assay is shown under metal-limited conditions (described in the main text). Total oligonucleotide produced from the 15-mer RNA substrate at the end of the assay period is shown. Data are normalized to the highest concentration of RNA synthesized.

excess. Optimal polymerization rates are achieved at low mM concentrations of divalent metal ions. Given that magnesium-citrate inhibits degradation, it would be expected that the chelate would also inhibit the polymerization activity. To test the effect of citrate on PNPase polymerization activity, we assayed the polymerization of ADP on an RNA substrate. At low concentrations of citrate, polymerization is inhibited, as expected (supplemental Fig. S4*a*).

Overall, our *in vitro* work suggests that PNPase is affected by the metabolite citrate. From our binding data, one high affinity site, potentially at the catalytic site, binds magnesium-chelated citrate to mediate an inhibitory effect on degradative activity. Support for metabolite binding sites within PNPase comes from structural studies discussed below.

Citrate in the PNPase Crystal Structure—The co-crystal of *E. coli* PNPase and RNA (30) was prepared in the presence of 200 mM citrate. In the 2.6 Å resolution structure (PDB code 3GCM) four molecules of citrate are seen bound to a PNPase

protomer. Two are found at the catalytic site (Fig. 4, *b* and *d*) and two are located at a distant vestigial site (Fig. 4, *b* and *e*).

At the catalytic site the citrate molecules occupy the proposed location of the catalytic intermediate (Fig. 4*c*). One of the molecules has the conformation observed in the small molecule crystal structure of magnesium-citrate, and occupies the binding site for the orthophosphate substrate in PNPase. The adjacent second citrate mimics the position of the scissile phosphate in the backbone of the RNA (Fig. 4*d*). At these positions the citrate molecules would be expected to prevent the formation of the Michaelis complex and provide a potential means of enzyme inhibition, in accord with the observed inhibitory effects seen *in vitro* (Fig. 3*b*). Under conditions in which citrate is magnesium-chelated, the metabolite inhibits both the forward and backwards reactions, *i.e.* degradation as well as polymerization.

Evidence for an Allosteric Regulation Pocket in PNPase—In addition to the magnesium-citrate and unchelated-citrate mol-
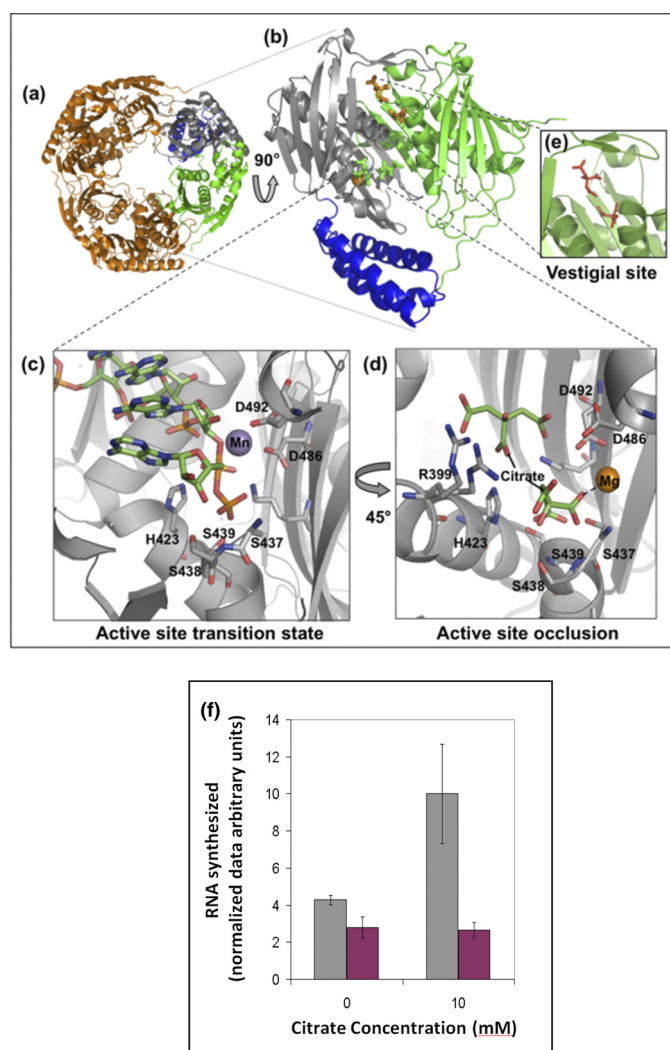
FIGURE 4. Metabolite-bound PNPase structure and evidence for an allosteric pocket. *a*, shown is the PNPase trimer enclosing the central channel, as viewed from above. One monomer is colored according to sub-domain structure as in *b*, and the other two monomers of the trimer are shown in *orange*. *b*, shown is the PNPase core monomer unit, as viewed from the side and colored according to subdomain structure with the N-terminal PH domain in *green*, the C-terminal PH domain in *gray*, and the helical domain in *blue*. Citrate is found at the vestigial active site (*orange*) and at the active site in Mg-chelated and free forms (*green*). Mg^{2+} is shown as an *orange sphere*. *c*, shown is an active site transition state model based on the PNPase core-manganese co-crystal structure (30). Shown is the active site within the RNase PH-domain (*gray*), catalytic Mn^{2+} (*purple sphere*), and modeled bound RNA (*orange* and *green*). *d*, shown is active site occlusion by citrate (*green*) and Mg-citrate (*green* and *orange sphere*) within the C-terminal RNase PH-domain (*gray*). *e*, citrate (*orange*) bound to the vestigial site within the N-terminal RNase PH-domain (*green*). *f*, analysis of the RNA substrate-based polymerization activity of PNPase parent (*gray*) and PNPase vestigial site mutant (*purple*) catalyzed by Mg^{2+} in the presence of varying citrate concentrations. Total oligonucleotide produced from the 15-mer RNA substrate at the end of the assay period are shown, normalized to the highest concentration of RNA synthesized. Data represent experimental repeat averages with S.D. indicated by *bars*.

ecules found in the active site, two free citrate molecules are located at a vestigial site in one of the three protomers of the crystallographic asymmetric unit (Fig. 4, *b* and *e*). This vestigial site is related to the true active site by internal structural duplication, and in the course of evolution it has lost capacity to catalyze phosphorolysis (44, 45). In this respect it is analogous to the evolutionarily conserved, phosphorolytically inactive archaeal and eukaryotic exosome subunits (46, 47). The func-

tion of these inactive sites remains unknown, and similarly, the role of the vestigial site in PNPase has not been established. The observation that the PNPase vestigial site binds citrate in a similar manner to the true active site indicates a capacity for regulatory metabolite binding.

Under our *in vitro* assay conditions, when citrate is predominantly in the metal-free form, polymerization of the substrate is enhanced (Fig. 3*c*). Correspondingly, at high concentrations of citrate (30–60 mM), the reverse process, *i.e.* degradation, is also enhanced (supplemental Fig. S4*b*). These activating effects are entirely the opposite of the inhibition seen under conditions in which magnesium-citrate may be the predominate species. It must be emphasized that the above results do not violate the principle of microscopic reversibility; instead, they suggest that citrate has two different binding sites; one where it is an inhibitor as the metal-bound form and one where it is an activator in its metal-free state. Evidence that the activating effect is due to binding at a distinct site comes from the observation that free citrate enhances the polymerization reactions catalyzed by manganese (Fig. 3*c*), whereas inhibition by metal-bound citrate depends upon the nature of the metal. Inhibition is observed in the presence of equimolar amounts of magnesium and citrate but not in the presence of equimolar amounts of manganese and citrate (Fig. 3*b*).

We suggest that the activating effects are due to free citrate bound at the vestigial site. The interactions of the vestigial site with citrate molecules are mediated by guanidinium groups of several arginines that are conserved in PNPase homologues. Mutations of the conserved vestigial site arginines Arg-153, Arg-372, Arg-405, and Arg-409 to alanine completely abolished the enhancement effect of free citrate (Fig. 4*f*). Nevertheless, this mutant is also inhibited by magnesium citrate (supplemental Fig. S5), just as seen for the wild-type enzyme (Fig. 3*b*), supporting the hypothesis that the metal-chelated citrate acts at a different location from the vestigial site; *e.g.* the active site.

These data indicate that the vestigial active site is a ligand binding allosteric pocket that responds to metal-free citrate. The binding of a ligand at the vestigial site may influence the location of a β-ribbon formed by residues 362–375 that is part of a central ring controlling the entry of RNA to the active site (30) and in this manner could influence substrate channeling to and from the catalytic site through an allosteric mechanism.

DISCUSSION

Decades of efforts to engineer metabolic pathways have revealed the complex behavior of metabolite concentrations and pathway fluxes in response to changing levels of enzymes. These observations illustrate how cellular metabolism requires regulation not only at the level of individual enzymes but also at a broader level that orchestrates the activities of many different enzymes distributed among branching pathways (48, 49). One possible contribution to such control might be post-transcriptional regulation, mediated through the regulatory effects of metabolites on ribonucleases.

We initially found that citrate could bind to PNPase after crystallization of PNPase core (30). Such binding could have been an artifact due to the high concentration of citrate present in the crystallization buffer. Here we present substantial evi-

dence that the Krebs cycle metabolite citrate does modulate the activity of the processive exoribonuclease PNPase *in vitro* and *in vivo* at physiological concentrations and that PNPase activities impact on the metabolome. Our findings suggest a key role for PNPase in the normal cellular response to citrate.

At the protein level, we show that the enzymatic activity of PNPase is inhibited in the presence of magnesium-chelated citrate, and we propose that this is due to its binding at, and occluding the catalytic site. The inhibition is observed at concentrations that correspond to physiological ranges (Ref. 43 and this study). In a cellular context, both magnesium homeostasis and citrate flux may in principle affect PNPase activity.

We also observe that PNPase activity is enhanced in the presence of free citrate and propose that this is due to binding at a vestigial site and acting as an allosteric regulator. Our mutagenesis data confirm that the vestigial active site mediates the response to free-citrate and could be an allosteric site. Metal-free citrate could be the natural ligand or it may mimic the effect of a natural regulatory ligand yet to be identified.

The ability to modulate PNPase activity through metabolite binding provides a mechanism for wide-ranging regulation of RNA transcript levels in response to changes in the cellular environment. Our microarray gene expression analyses demonstrate that many transcripts are affected in a PNPase-mediated response to citrate. Inhibition of the degradative activity by magnesium-chelated citrate is anticipated to stabilize certain transcripts and decay intermediates or re-route the degradation through hydrolytic pathways, which are perhaps most costly in terms of product recycling. The impact of PNPase activity upon gene expression is likely to result in changes in the proteome, which in turn will result in changes in the metabolome. We show that cells lacking PNPase or degradosome-coupled PNPase activities differ in their metabolite concentrations when compared with parental strains. The other canonical components of the degradosome also seem to be involved in regulation of the metabolome in response to environmental change (see the data for the null mutant of the DEAD-box helicase RhlB and parent in supplemental Table S4 and Fig. S6). This indicates that the activities of RNA degradative machines impact upon metabolic control.

Taken together our results support a link between the cellular metabolic status and RNA degradative activity. Metabolites impact on ribonuclease function, and this has a wide ranging impact on many transcripts, which in turn regulates the cellular proteome and metabolome. Finally, changes in the metabolome can feed back to modulate ribonuclease activity.

The metabolite-mediated PNPase effect shown here for *E. coli* is potentially conserved in PNPase homologues found in archaea and eukaryotes. Human PNPase regulates RNA import in the mitochondria (50), the location of the Krebs cycle, where citrate is present at low mM concentrations, comparable with the concentrations used in our studies. In addition, the PNPase vestigial site of unknown function, now proposed to be involved in responding to citrate or other metabolites, is evolutionarily conserved in the phosphorolytically inactive archaeal and eukaryotic exosome subunits (46, 47). A combination of wide ranging control by PNPase and the degradosome and the direct or indirect effects of metabolites on their constituent activities

represents a hitherto unrecognized integrative control mechanism that regulates homeostasis and response to environmental change.

*Note Added in Proof—*A recent report identifies PNPase as a direct target of the messenger cyclic diguanylic acid in *E. coli* (51).

REFERENCES

1. Mohanty, B. K., and Kushner, S. R. (2000) *Proc. Natl. Acad. Sci. U.S.A.* **97,** 11966–11971
2. Schuster, G., and Stern, D. (2009) *Prog. Mol. Biol. Transl. Sci.* **85,** 393–422
3. Clements, M. O., Eriksson, S., Thompson, A., Lucchini, S., Hinton, J. C., Normark, S., and Rhen, M. (2002) *Proc. Natl. Acad. Sci. U.S.A.* **99,** 8784–8789
4. Ygberg, S. E., Clements, M. O., Rytkönen, A., Thompson, A., Holden, D. W., Hinton, J. C., and Rhen, M. (2006) *Infect Immun.* **74,** 1243–1254
5. Yang, J., Jain, C., and Schesser, K. (2008) *J. Bacteriol.* **190,** 3774–3778
6. Andrade, J. M., and Arraiano, C. M. (2008) *RNA* **14,** 543–551
7. Awano, N., Inouye, M., and Phadtare, S. (2008) *J. Bacteriol.* **190,** 5924–5933
8. Cheng, Z. F., and Deutscher, M. P. (2003) *Proc. Natl. Acad. Sci. U.S.A.* **100,** 6388–6393
9. Deutscher, M. P. (2006) *Nucleic Acids Res.* **34,** 659–666
10. Mohanty, B. K., and Kushner, S. R. (2003) *Mol. Microbiol.* **50,** 645–658
11. Mohanty, B. K., and Kushner, S. R. (2006) *Nucleic Acids Res.* **34,** 5695–5704
12. Slomovic, S., Portnoy, V., Yehudai-Resheff, S., Bronshtein, E., and Schuster, G. (2008) *Biochim. Biophys. Acta* **1779,** 247–255
13. Viegas, S. C., Pfeiffer, V., Sittka, A., Silva, I. J., Vogel, J., and Arraiano, C. M. (2007) *Nucleic Acids Res.* **35,** 7651–7664
14. Carpousis, A. J. (2007) *Annu. Rev. Microbiol.* **61,** 71–87
15. Marcaida, M. J., DePristo, M. A., Chandran, V., Carpousis, A. J., and Luisi, B. F. (2006) *Trends Biochem. Sci* **31,** 359–365
16. Callaghan, A. J., Aurikko, J. P., Ilag, L. L., Günter Grossmann, J., Chandran, V., Kühnel, K., Poljak, L., Carpousis, A. J., Robinson, C. V., Symmons, M. F., and Luisi, B. F. (2004) *J. Mol. Biol.* **340,** 965–979
17. Callaghan, A. J., Marcaida, M. J., Stead, J. A., McDowall, K. J., Scott, W. G., and Luisi, B. F. (2005) *Nature* **437,** 1187–1191
18. Py, B., Higgins, C. F., Krisch, H. M., and Carpousis, A. J. (1996) *Nature* **381,** 169–172
19. Khemici, V., Poljak, L., Luisi, B. F., and Carpousis, A. J. (2008) *Mol. Microbiol.* **70,** 799–813
20. Bernstein, J. A., Lin, P. H., Cohen, S. N., and Lin-Chao, S. (2004) *Proc. Natl. Acad. Sci. U.S.A.* **101,** 2758–2763
21. Lopez, P. J., Marchand, I., Joyce, S. A., and Dreyfus, M. (1999) *Mol. Microbiol.* **33,** 188–199
22. Morita, T., Kawamoto, H., Mizota, T., Inada, T., and Aiba, H. (2004) *Mol. Microbiol.* **54,** 1063–1075
23. Chandran, V., and Luisi, B. F. (2006) *J. Mol. Biol.* **358,** 8–15
24. Erce, M. A., Low, J. K., March, P. E., Wilkins, M. R., and Takayama, K. M. (2009) *Biochim. Biophys. Acta* **1794,** 1107–1114
25. Hardwick, S. W., Chan, V. S., Broadhurst, R. W., and Luisi, B. F. (2011) *Nucleic Acids Res.* **39,** 1449–1459
26. Commichau, F. M., Rothe, F. M., Herzberg, C., Wagner, E., Hellwig, D.,

Lehnik-Habrink, M., Hammer, E., Völker, U., and Stülke, J. (2009) *Mol. Cell. Proteomics* **8,** 1350 –1360

27. Del Favero, M., Mazzantini, E., Briani, F., Zangrossi, S., Tortora, P., and Dehò, G. (2008) *J. Biol. Chem.* **283,** 27355–27359

28. Gatewood, M. L., and Jones, G. H. (2010) *J. Bacteriol.* **192,** 4275– 4280

29. Siculella, L., Damiano, F., di Summa, R., Tredici, S. M., Alduina, R., Gnoni, G. V., and Alifano, P. (2010) *Mol. Microbiol.* **77,** 716 –729

30. Nurmohamed, S., Vaidialingam, B., Callaghan, A. J., and Luisi, B. F. (2009) *J. Mol. Biol.* **389,** 17–33

31. Khemici, V., Toesca, I., Poljak, L., Vanzo, N. F., and Carpousis, A. J. (2004) *Mol. Microbiol.* **54,** 1422–1430

32. Leroy, A., Vanzo, N. F., Sousa, S., Dreyfus, M., and Carpousis, A. J. (2002) *Mol. Microbiol.* **45,** 1231–1243

33. Le Belle, J. E., Harris, N. G., Williams, S. R., and Bhakoo, K. K. (2002) *NMR Biomed.* **15,** 37– 44

34. Atherton, H. J., Gulston, M. K., Bailey, N. J., Cheng, K. K., Zhang, W., Clarke, K., and Griffin, J. L. (2009) *Mol. Syst. Biol.* **5,** 259

35. Pears, M. R., Cooper, J. D., Mitchison, H. M., Mortishire-Smith, R. J., Pearce, D. A., and Griffin, J. L. (2005) *J. Biol. Chem.* **280,** 42508 – 42514

36. Stickney, L. M., Hankins, J. S., Miao, X., and Mackie, G. A. (2005) *J. Bacteriol.* **187,** 7214 –7221

37. Studier, F. W. (2005) *Protein Expr. Purif.* **41,** 207–234

38. Worrall, J. A., Górna, M., Crump, N. T., Phillips, L. G., Tuck, A. C., Price, A. J., Bavro, V. N., and Luisi, B. F. (2008) *J. Mol. Biol.* **382,** 870 – 883

39. Donovan, W. P., and Kushner, S. R. (1986) *Proc. Natl. Acad. Sci. U.S.A.* **83,** 120 –124

40. Donovan, W. P., and Kushner, S. R. (1983) *Nucleic Acids Res.* **11,** 265–275

41. Cheng, Z. F., Zuo, Y., Li, Z., Rudd, K. E., and Deutscher, M. P. (1998) *J. Biol. Chem.* **273,** 14077–14080

42. Ishii, N., Nakahigashi, K., Baba, T., Robert, M., Soga, T., Kanai, A., Hirasawa, T., Naba, M., Hirai, K., Hoque, A., Ho, P. Y., Kakazu, Y., Sugawara, K., Igarashi, S., Harada, S., Masuda, T., Sugiyama, N., Togashi, T., Hasegawa, M., Takai, Y., Yugi, K., Arakawa, K., Iwata, N., Toya, Y., Nakayama, Y., Nishioka, T., Shimizu, K., Mori, H., and Tomita, M. (2007) *Science* **316,** 593–597

43. Bennett, B. D., Kimball, E. H., Gao, M., Osterhout, R., Van Dien, S. J., and Rabinowitz, J. D. (2009) *Nat. Chem. Biol.* **5,** 593–599

44. Symmons, M. F., Jones, G. H., and Luisi, B. F. (2000) *Structure* **8,** 1215–1226

45. Symmons, M. F., Williams, M. G., Luisi, B. F., Jones, G. H., and Carpousis, A. J. (2002) *Trends Biochem. Sci.* **27,** 11–18

46. Liu, Q., Greimann, J. C., and Lima, C. D. (2006) *Cell* **127,** 1223–1237

47. Schmid, M., and Jensen, T. H. (2008) *Trends Biochem. Sci.* **33,** 501–510

48. Daran-Lapujade, P., Rossell, S., van Gulik, W. M., Luttik, M. A., de Groot, M. J., Slijper, M., Heck, A. J., Daran, J. M., de Winde, J. H., Westerhoff, H. V., Pronk, J. T., and Bakker, B. M. (2007) *Proc. Natl. Acad. Sci. U.S.A.* **104,** 15753–15758

49. Hardiman, T., Lemuth, K., Keller, M. A., Reuss, M., and Siemann-Herzberg, M. (2007) *J. Biotechnol.* **132,** 359 –374

50. Wang, G., Chen, H. W., Oktay, Y., Zhang, J., Allen, E. L., Smith, G. M., Fan, K. C., Hong, J. S., French, S. W., McCaffery, J. M., Lightowlers, R. N., Morse, H. C., 3rd, Koehler, C. M., and Teitell, M. A. (2010) *Cell* **142,** 456 – 467

51. Tuckerman, J. R., Gonzalez, G., and Gilles-Gonzalez, M. A. (2011) *J. Mol. Biol.*, in press